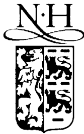
ELSEVIER

Nuclear Instruments and Methods in Physics Research B 175–177 (2001) 187–192

NIM B Beam Interactions with Materials & Atoms

www.elsevier.nl/locate/nimb

Properties of InAs nanocrystals in silicon formed by sequential ion implantation

A.L. Tchebotareva [a,*], J.L. Brebner [a], S. Roorda [a], C.W. White [b]

[a] *Research Group on the Physics and Technology of Thin Films (GCM), Physics Department, Université de Montréal, Montreal, Que., Canada H3C 3J7*

[b] *Oak Ridge National Laboratory, Oak Ridge, USA*

Abstract

Optical and structural properties of InAs nanocrystals fabricated by co-implantation of In and As ions in Si-c(1 0 0), followed by thermal annealing are investigated. In the first sample named Si/AsIn the implantation of As ions was followed by In ion implantation, whereas in the second sample named Si/InAs the order of implantation was inverted. RBS spectra of these samples taken before and after annealing show that the depth profiles of implanted ions depend strongly on the order of implantation. XRD measurements confirm the presence of InAs crystallites oriented along the crystallographic axes of the silicon matrix irrespective of the order of implantation. Low-temperature photoluminescence measurements show a large PL band in the region 0.83–1.03 eV for the sample Si/AsIn. No PL was observed in the sample Si/InAs. The optical absorption spectrum of Si/AsIn sample shows a large absorption band in the region 0.4–0.9 eV, whereas the spectrum of sample Si/InAs contains two distinct absorption bands at 0.45 eV and 0.8 eV. This may indicate a bimodal distribution of sizes of InAs nanocrystals in the Si/InAs sample. The absorption and photoluminescence bands arise from the blueshifted bandgap absorption/emission of InAs nanocrystals, this blueshift being dependent on the size of the nanocrystals. These results indicate that in the case of As ions implanted first, the InAs nanocrystals are smaller than for the case of In ions implanted first. This effect may be explained by the low solubility of In ions in the silicon matrix, which results in agglomeration of In ions during the implantation. When As ions are implanted afterwards, the In clusters are partially transformed into InAs nanocrystals which grow in size during the annealing. Hence, the order of ion implantation is found to influence the size and distribution of the resultant nanocrystals, as well as the optical properties of the samples obtained. © 2001 Elsevier Science B.V. All rights reserved.

PACS: 61.82.Rx; 36.40.Mr; 61.72.Tt; 36.40.Vz
Keywords: InAs nanocrystals; Sequential ion implantation; XRD; Photoluminescence

1. Introduction

Nanocrystals of semiconductor compounds have been extensively studied during last decade because of their peculiar optical properties. These are mostly due to quantum confinement effects that

* Corresponding author. Tel.: +1-514-343-6111/1603; fax: +1-514-343-2071.
E-mail address: tchebota@ere.umontreal.ca (A.L. Tchebotareva).

0168-583X/01/$ - see front matter © 2001 Elsevier Science B.V. All rights reserved.
PII: S 0 1 6 8 - 5 8 3 X (0 0) 0 0 6 6 0 - 1

arise when the size of a semiconductor nanocrystal is comparable with or smaller than the bulk exciton radius of the semiconductor. Since the bulk exciton radius of III–V class semiconductors is larger than that of II–VI semiconductors [1], the quantum confinement effects are more pronounced in nanocrystals of III–V compounds. Due to quantum confinement, the energy band structure is modified, and the bandgap energy E_g comes to be a function of the size of nanocrystal [2]. When a nanocrystal becomes smaller the associated bandgap E_g increases, thus manifesting a blue shift [2]. Consequently, the absorption and related optical properties of semiconductor nanocrystals are strongly affected by their size. As a result, it becomes possible to tune the absorption and emission wavelengths of a material by creating in this material semiconductor nanocrystals of an appropriate size. In order to synthesize nanocrystals with desired optical properties it is therefore important to control their average size and size distribution.

One technique allowing the formation of many types of nanocrystals inside different solid substrates is ion implantation followed by a thermal annealing [3–18]. Modifying the regime of annealing or changing the order in which different ion species are implanted provides an efficient way of controlling the sizes of compound nanocrystals thus formed. It has been shown that nanocrystals of group VI semiconductors, several II–VI semiconductors, and most of the III–V semiconductor compounds can be produced by this technique in amorphous SiO_2, as well as in crystalline Si and Al_2O_3 substrates [3–18].

In the present work we study structural and optical properties of InAs nanocrystals synthesized in crystalline Si(1 0 0) substrate by sequential implantation of In^+ and As^+ ions. We show that for the same annealing regime, a change of the order of implantation of two ion species leads to considerable differences in structural and optical properties of the obtained samples.

2. Sequential ion implantation: structural properties

Single-crystalline Si(1 0 0) samples were implanted with In^+ and As^+. For each type of ion the fluence implanted was 10^{17} cm^{-2}. The energies of In^+ and As^+ ions were 800 keV and 500 keV, respectively. The projected ranges for ions of these energies, as predicted by TRIM simulations, were $R_p(In^+) = 3180$ Å and $R_p(As^+) = 3102$ Å, so that one would expect the concentration profiles of these two ions to be centered at about the same depth. All of the implantations were carried out at the temperature $T = 500°C$ so as to better preserve the crystallinity of the substrate. Two kinds of samples were prepared. Samples of the first kind (identified as Si/AsIn) were implanted with the As^+ ions first and the In^+ ions afterwards. In the second kind of samples (referred to as Si/InAs) the order of implantation of the two ion species was inverted. After implantation, the samples were annealed in a reduced atmosphere ($Ar + 4\%H_2$) at 800°C during 1 h and later at 900°C during 1 h.

The structural properties of the samples were investigated using X-ray diffraction (XRD), Rutherford backscattering (RBS), and Transmission electron microscopy (TEM) techniques. XRD measurements were performed using a high-resolution diffractometer system equipped with a four-crystal monochromator. XRD spectra of the as implanted samples of each type did not reveal any peak corresponding to crystalline InAs. However, in the spectra of both Si/AsIn and Si/InAs samples a peak due to In was observed. After the second annealing the X-ray patterns of both Si/AsIn and Si/InAs samples clearly displayed the (0 0 4) and (0 0 2) crystalline InAs peaks as well as the In peak (see Fig. 1(a,b)). These indicate that the InAs nanocrystals are aligned along the crystallographic axes of the Si matrix, which agrees with the results of White et al. [18]. The measurements suggested that no InAs in crystalline form appeared in the as implanted state. However, the quantity of crystalline In in the samples in this state was considerable. After the annealing some crystalline InAs was formed in both types of samples, and at the same time the quantity of crystalline In decreased. Moreover, the XRD data of Fig. 1(b) suggest that when In is implanted first, less crystalline InAs is formed and more crystalline In remains in the sample.

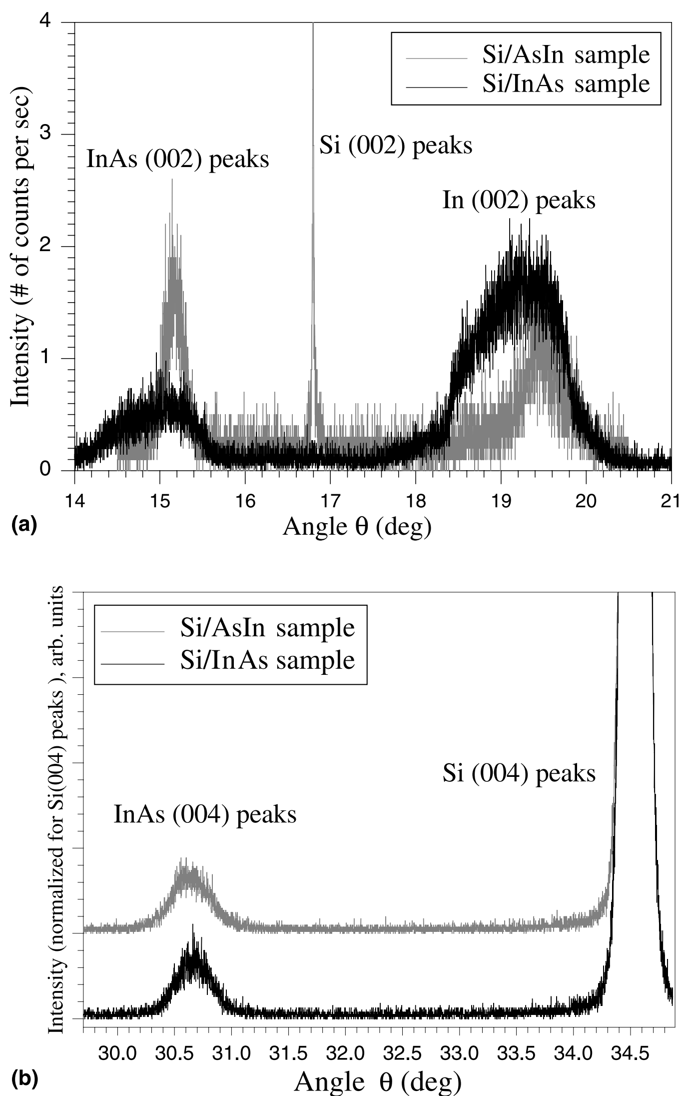

Fig. 1. XRD spectra of the samples after the second annealing (at 900°C): (a) region of (0 0 2) peaks; (b) region of (0 0 4) peaks.

The RBS measurements using 2 MeV He^+ ions were carried out on the samples in the as implanted state as well as after each annealing. Typical spectra for the as implanted samples are shown in the Fig. 2(a,b). The difference between the RBS spectra of the two types of samples is seen to be considerable. In the spectrum of Si/InAs sample a sharp peak corresponding to In ions is present, as well as a broad peak corresponding to As ion distribution. Such a narrow distribution of In after the end of implantation may be consequent on a segregation of In and formation of In crystallites in the sample. The spectrum of Si/AsIn sample contains two broad peaks due to In and As ion distributions. Analysis of these spectra, as well as of other spectra recorded at different scattering angles, allowed us to establish the distributions of In and As ions (they are not shown here). Significant deviations from a standard implantation profile were observed, as could be expected for such high dose

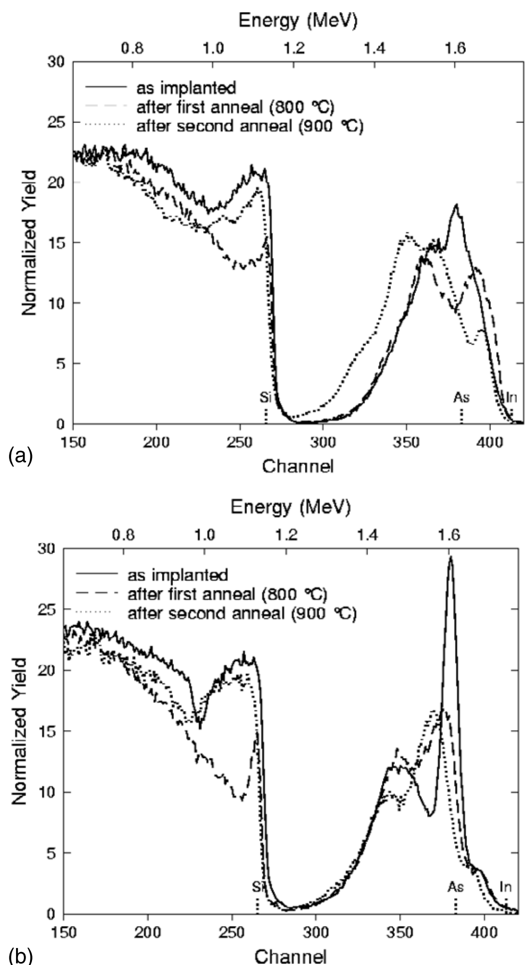

Fig. 2. RBS spectra of the samples before and after annealings. The dashed vertical lines denote the surface levels of Si, As and In atoms. (a) Si/AsIn sample (As^+ implanted first). (b) Si/InAs sample (In^+ implanted first).

heavy ion implants. However, most implanted species were confined to a ~400 nm thick surface layer with partial overlap of the As and In profiles of as implanted samples (see Fig. 2(a,b)). The first annealing (at 800°C) led to almost complete overlap of the depth distributions of the two ion species, the peaks due to In and As ions being separated by the same energy as the surface levels of these atoms (see Fig. 2(a,b)). Such redistribution may indicate a formation of InAs compound as a result of the annealing. After the second annealing (at 900°C) some special separation between In and As ions was observed (see Fig. 2(a,b)).

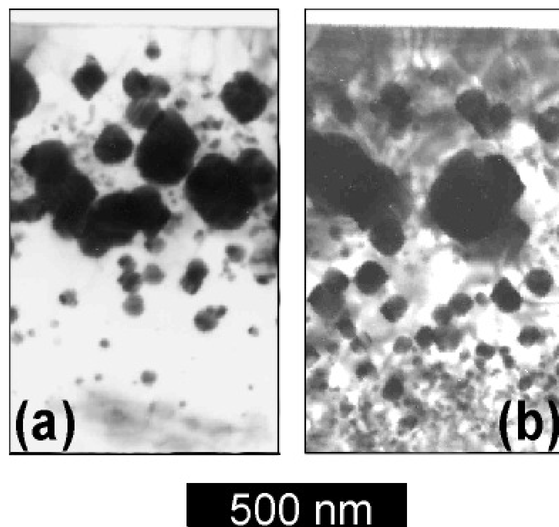

Fig. 3. TEM of implanted samples after the second annealing (at 900°C). (a) Si/AsIn sample. (b) Si/InAs sample.

In addition, the TEM measurements have been performed on both Si/AsIn and Si/InAs samples. The micrographs so obtained (see Fig. 3(a,b)) showed the presence of facetted InAs nanocrystals. The crystals are located under the substrate's surface within a layer of about 350–400 nm thick. Their sizes vary from ~10 nm to ~100 nm, with an average size of 70 nm for the case of Si/AsIn sample. [1] Nanocrystals created in Si/InAs sample have a bimodal size distribution with central sizes of 64 and 160 nm. [1]

3. Sequential ion implantation: optical properties

The infrared absorption of samples before and after annealings was studied at a temperature $T = 9 \pm 2$ K. In the as implanted samples no absorption bands were observed up to the crystalline Si bandgap absorption energy. After the first annealing two absorption bands appeared in the spectra of both samples (see Fig. 4(a)). The ab-

[1] These are preliminary values only.

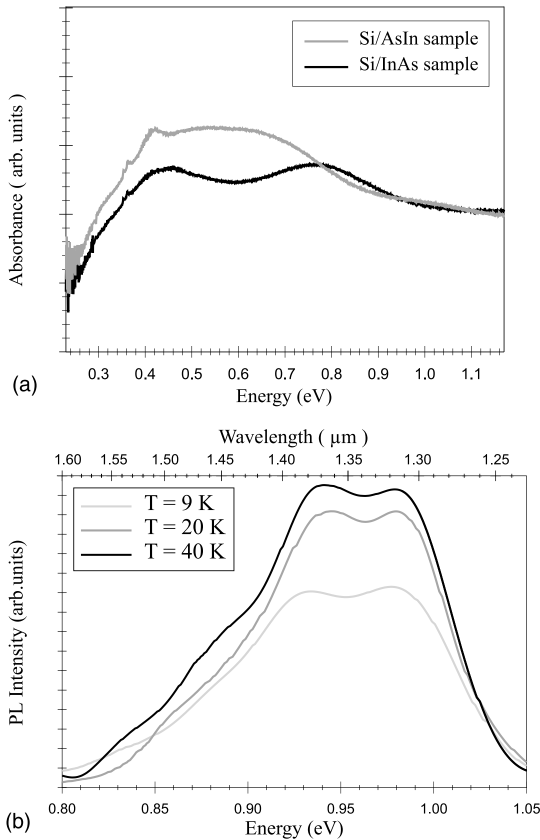

Fig. 4. (a) IR absorption spectra of Si/AsIn and Si/InAs annealed samples. (b) Photoluminescence spectra of Si/AsIn sample after the second annealing (at 900°C).

sorption spectrum of sample Si/AsIn shows a large band in the region 0.4–0.8 eV, whereas the spectrum of sample Si/InAs contains two distinct absorption bands at 0.45 eV and 0.9 eV. This may indicate a bimodal size distribution of the absorbing nanocrystals. Second annealing did not induce any considerable changes in the shape of absorption spectra of samples.

Low-temperature photoluminescence (PL) was investigated by use of a tunable Ti:sapphire laser beam at wavelength $\lambda_0 = 800$ nm. The PL spectrum of the Si/AsIn sample obtained after the second annealing contained a large band in the region 0.83–1.03 eV. The intensity of this band increased when the temperature increased from 10 to 40 K, as shown in Fig. 4(b), and decreased at higher temperatures. No PL was observed in the Si/InAs sample.

4. Discussion and conclusion

There exists a considerable difference between Si/AsIn and Si/InAs samples. This points to a significant atomic mobility during the ion implantation. The XRD, RBS and TEM measurements performed before and after annealings suggest that the equilibrium solubilities and diffusivities of In and As in Si play a crucial role in the formation of InAs nanocrystalline structures. In the sample where As^+ was implanted first, the relatively low diffusivity and higher solubility of As^+, as compared to In^+, favour the implanted species to be distributed atomically or at most in very small aggregates. Addition of In^+ during the second implantation can then lead directly to the nucleation of InAs nanocrystals. Consequently, in the sample where In^+ ions were implanted first, the higher diffusivity and lower solubility led to the formation of In nanocrystals even before the In implantation had terminated. Subsequently implanted As^+ ions may thus form InAs nanocrystals either directly from In that still remains in solution, or through conversion of In nanocrystals to InAs nanocrystals. Hence, there are two distinct mechanisms of the formation of InAs nanocrystals, which leads to a strongly bimodal size distribution.

The PL signal from the Si/AsIn sample appears to come from the InAs nanocrystals. However, further measurements are needed to exclude other possible sources. The absence of PL signal from the Si/InAs sample is likely to be due to a very large number of extended defects in this sample, whose origins are not yet clearly understood.

Our results show that InAs nanocrystals can be formed by sequential ion implantation in Si(1 0 0) irrespective of the order of the implantation of ion species. Whichever the order of implantation, the nanocrystals obtained are facetted and aligned along the crystallographic axes of the substrate. However, the sequence of implantation determines the size distribution of nanocrystals and optical properties of the samples obtained.

Acknowledgements

Authors are grateful to Prof. P. Desjardins for the expert assistance with the TEM measurements and fruitful discussions, and to Prof. R. Leonelli for the help with PL measurements. We would also like to acknowledge P. Berichon and R. Gosselin for the assistance with the TANDETRON accelerator and V. Pagé for the assistance with preparations of samples for TEM.

This work is financially supported by the Natural Sciences and Engineering Research Council of Canada (NSERC), the Fonds pour la Formation des Chercheurs et Aide à la Recherche du Québec (FCAR), and US Department of Energy under contract DE-AC05-00OR22725 with the Oak Ridge National Laboratory, managed by UT-Battelle, LLC.

References

[1] M.A. Olshavsky, A.N. Goldstein, A.P. Alivisatos, J. Am. Chem. Soc. 112 (1990) 9438.
[2] U. Woggon, Optical Properties of Semiconductor Nanocrystals, Springer Tracts in Modern Physics, Vol. 36, Springer, Berlin, 1997.
[3] P. Madakson, E. Ganin, J. Karasinski, J. Appl. Phys. 67 (1990) 4053.
[4] S.Yu. Shiryaev, A. Nylandsted Larsen, M. Deicher, J. Appl. Phys. 72 (1994) 410.
[5] S.Yu. Shiryaev, A. Nylandsted Larsen, Nucl. Instr. and Meth. B 80/81 (1992) 846.
[6] H. Atwater, K.V. Shcheglov, S.S. Wong, K.J. Vahala, R.C. Flagan, M.L. Brongersma, A. Polman, Mater. Res. Soc. Symp. Proc. 316 (1994) 409.
[7] T. Shimizu-Iwayama, K. Fujita, S. Nakao, K. Saitoh, T. Fujita, N. Itoh, J. Appl. Phys. 75 (1994) 7779.
[8] J.G. Zhu, C.W. White, J.D. Budai, S.P. Withrow, Y. Chen, Mater. Res. Soc. Symp. Proc. 358 (1995) 175.
[9] J.G. Zhu, C.W. White, J.D. Budai, S.P. Withrow, Y. Chen, J. Appl. Phys. 77 (1995) 4386.
[10] K.S. Min, K.Y. Shcheglov, C.M. Yang, H.A. Atwater, M.L. Brongersma, A. Polman, Appl. Phys. Lett. 68 (1996) 2511.
[11] W. Skorupa, R.A. Yankov, I.E. Tyschenko, H. Frob, T. Bohme, K. Leo, Appl. Phys. Lett. 68 (1996) 2410.
[12] C.W. White, J.D. Budai, J.G. Zhu, S.P. Withrow, D.M. Hembree, D.O. Henderson, A. Ueda, Y.S. Tung, R. Mu, Mater. Res. Soc. Symp. Proc. 396 (1996) 377.
[13] K.S. Min, K.V. Shcheglov, C.M. Yang, H.A. Atwater, M.L. Brongersma, A. Polman, Appl. Phys. Lett. 69 (1996) 2033.
[14] P. Mutti, G. Ghislotti, S. Bertoni, L. Bonoldi, G.F. Cerofolini, L. Meda, E. Grilli, M. Guzzi, Appl. Phys. Lett. 66 (1995) 851.
[15] C.W. White, J.D. Budai, J.G. Zhu, S.P. Withrow, S.J. Pennycook, D.M. Hembree, D.S. Zhou, T. Yo-Dihn, R.H. Magruder, Mater. Res. Soc. Symp. Proc. 316 (1994) 487.
[16] C.W. White, J.D. Budai, J.G. Zhu, S.P. Withrow, R.A. Zuhr, D.M. Hembree, D.O. Henderson, A. Ueda, Y.S. Tung, R. Um, R.H. Magruder, J. Appl. Phys. 79 (1996) 1876.
[17] R.H. Magruder, J.E. Witting, R.A. Zuhr, J. Non-Cryst. Solids 163 (1993) 162.
[18] C.W. White, J.D. Budai, S.P. Withrow, J.G. Zhu, S.J. Pennycook, R.A. Zuhr, D.M. Hembree Jr., D.O. Henderson, R.H. Magruder, M.J. Yakaman, G. Mondragon, S. Prawer, Nucl. Instr. and Meth. B 127/128 (1997) 545.